sustainability

MDPI

Article

Study of Ecosystem Degradation Dynamics in the Peruvian Highlands: Landsat Time-Series Trend Analysis (1985–2022) with ARVI for Different Vegetation Cover Types

Deyvis Cano [1,*], Samuel Pizarro [2], Carlos Cacciuttolo [3,*], Richard Peñaloza [4], Raúl Yaranga [5] and Marcelo Luciano Gandini [6]

1 Programa Académico de Ingeniería Ambiental, Universidad de Huánuco, Huánuco 10003, Peru
2 Dirección de Desarrollo Tecnológico Agrario, Instituto Nacional de Innovación Agraria (INIA), Carretera Saños Grande-Hualahoyo Km 8 Santa Ana, Huancayo 12002, Peru; agpres_santaana@inia.gob.pe
3 Department of Civil Works and Geology, Catholic University of Temuco, Temuco 4780000, Chile
4 Environmental Science & Health—ESH Research Group, Facultad de Medicina Humana, Universidad Nacional del Centro del Perú, Av. Mariscal Castilla N° 3909, Huancayo 12006, Peru; rpenhaloza@uncp.edu.pe
5 Andean Ecosystem Research Group, Facultad de Zootecnia, Universidad Nacional del Centro del Perú, Av. Mariscal Castilla 3089, Huancayo, Junin 12002, Peru; ryaranga@uncp.edu.pe
6 Laboratorio de Investigación y Servicios en Teledetección, Facultad de Agronomía, NUCEVA, Universidad Nacional del Centro de la Provincia de Buenos Aires, Av. República de Italia 780, Azul 7300, Argentina; mgandini@faa.unicen.edu.ar
* Correspondence: deyvis.cano@udh.edu.pe (D.C.); ccacciuttolo@uct.cl (C.C.)

Abstract: The high-Andean vegetation ecosystems of the Bombón Plateau in Peru face increasing degradation due to aggressive anthropogenic land use and the climate change scenario. The lack of historical degradation evolution information makes implementing adaptive monitoring plans in these vulnerable ecosystems difficult. Remote sensor technology emerges as a fundamental resource to fill this gap. The objective of this article was to analyze the degradation of vegetation in the Bombón Plateau over almost four decades (1985–2022), using high spatiotemporal resolution data from the Landsat 5, 7, and 8 sensors. The methodology considers: (i) the use of the atmosphere resistant vegetation index (ARVI), (ii) the implementation of non-parametric Mann–Kendall trend analysis per pixel, and (iii) the affected vegetation covers were determined by supervised classification. This article's results show that approximately 13.4% of the total vegetation cover was degraded. According to vegetation cover types, bulrush was degraded by 21%, tall grass by 18%, cattails by 16%, wetlands by 14%, and puna grass by 13%. The Spearman correlation ($p < 0.01$) determined that degraded covers are replaced by puna grass and change factors linked with human activities. Finally, this article concludes that part of the vegetation degradation is related to anthropogenic activities such as agriculture, overgrazing, urbanization, and mining. However, the possibility that environmental factors have influenced these events is recognized.

Keywords: degradation; high-Andean vegetation; ARVI; Mann–Kendall; Landsat 5, 7 and 8; remote sensing

check for updates

Citation: Cano, D.; Pizarro, S.; Cacciuttolo, C.; Peñaloza, R.; Yaranga, R.; Gandini, M.L. Study of Ecosystem Degradation Dynamics in the Peruvian Highlands: Landsat Time-Series Trend Analysis (1985–2022) with ARVI for Different Vegetation Cover Types. *Sustainability* **2023**, *15*, 15472. https://doi.org/10.3390/su152115472

Academic Editors: Jing Wei, Hong Tang and Naisen Yang

Received: 6 October 2023
Revised: 25 October 2023
Accepted: 26 October 2023
Published: 31 October 2023

1. Introduction

The vegetation in high-Andean ecosystems mainly comprises plant communities such as tall grass, puna grass, wetlands, bulrush, and cattails, among others. They occupy a large part of the territory of the Andes and constitute a valuable resource for the population's survival and biodiversity. These make up complex, fragile, and essential spaces in regulating the climate, the water cycle, carbon capture, productivity, the conservation of biodiversity, and other ecosystem services [1]. The Bombón Plateau, in the Junín region in Peru, is home to high biodiversity and a large number of species of high-Andean flora and fauna that are endemic and adapted to the humid puna climate. It is home to Lake Junín, the second-largest lake in Peru. It is in this place where the Mantaro River basin originates, one of the most significant water contributors to the Amazon basin [2,3]. Likewise, in this place, agricultural, livestock, urban expansion, and mining activities are carried out that constantly contribute to the degradation of vegetation and, consequently, to the alteration of these ecosystems. Similarly, nearby anthropogenic activities such as open-pit mining and metallurgy generate atmospheric pollution by heavy metals [4] in combination with anomalies of environmental factors such as temperature, precipitation, and evapotranspiration, altering plant dynamics over time [5,6]. Although the importance and fragility of these ecosystems are recognized, the degradation of high-Andean vegetation and its environmental, economic, and social consequences have not received adequate attention for formulating adaptive monitoring plans [7].

Precisely, it is possible to identify changes in coverage over time through remote sensors, automatic classification algorithms, and field validation data. Few studies have evaluated land-cover or land-use changes using remote sensing in the central Andes of Peru [8–10]. Likewise, remote sensors are being used worldwide to evaluate vegetation degradation through indices. These evaluations are limited to short analysis periods with uninterrupted and low spatial resolution sensors (e.g., MODIS and GIMMS). Currently, the analysis of pixel-by-pixel degradation through the evaluation of the trend of vegetation indices to determine the deterioration or improvement of vegetation for considerable periods is made possible through the Google Earth Engine platform (GEE) [11,12]. Thanks to this platform, it is possible to use large amounts of data and complement products such as those of the Landsat remote sensor series (Landsat 5, 7, and 8). This fact makes it possible to access high-quality spatial and temporal resolution images, for land-use change analysis and vegetation degradation analysis [13,14].

The atmosphere resistant vegetation index (ARVI) is characterized by minimizing aerosol's effect due to the blue band's influence [15]. This type of inconvenience when monitoring vegetation is widely observed in arid and semi-arid areas such as Andean ecosystems. Likewise, this index shows advantages in its application by providing information on the photosynthetic pigment of the plant, specifically on chlorophyll and carotenoids; it shows sensitivity when the plant canopy is variable by reducing the influence of the leaf surface and its internal structure. In addition, it has demonstrated good performance in determining the development, productivity, biomass, growth, and vegetation in arid areas [16,17]. Precisely, these advantages allow for the evaluation of the trend of vegetation indices in terms of space and length of time and reflect the evolution and direction of vegetation, and change, whether negative or positive, providing essential, spatial, and temporal information on vegetation degradation [18,19].

The absence of research that spatially and temporally analyzes the state and dynamics of high-Andean vegetation raises the need to deepen its understanding through the use of remote sensors. Furthermore, the importance of using tools to generate essential information that supports the formulation of adaptive management plans to improve adequate care in these spaces leads us to raise the following questions:

(i) What is the extent and location of degraded plant areas on the Bombón Plateau, Junín, Peru, during the period 1985–2022?
(ii) What are the patterns and trends of degradation, how have they evolved, and what are the factors and processes of substitution of the affected vegetation cover types?
(iii) How has human activity influenced changes in vegetation and what are the implications of these degradation patterns for vegetation management and conservation?

Therefore, the central objective of this study is to evaluate the magnitude of plant degradation in the Bombón Plateau, Junín, Peru, over an extended period of almost four decades (1985–2022), taking advantage of the high spatial and temporal resolution data provided by Landsat sensors 5, 7, and 8. By applying the ARVI, non-parametric Mann–Kendall trend analysis, and an annual supervised classification, this study seeks to:

(i) Delineate and quantify the extent of degraded plant areas during the period studied.
(ii) Decipher the dynamics and replacement patterns of the affected vegetation covers.

(iii) Examine land-use changes resulting from anthropogenic activities such as agriculture, mining, and urban expansion.

With these objectives, we seek to provide a comprehensive understanding of the patterns of vegetation degradation, the extent of vegetation cover type in the study area, and how human activities have influenced these changes over time. The work represents a vital tool in adaptive management in the identification of priority conservation and management areas based on interactions with both extension cover types and vegetation degradations. The findings have notable implications for understanding the changing dynamics of vegetal degraded communities in high-Andean areas.

2. Materials and Methods

2.1. Study Zone

The Bombón Plateau is in the Peruvian Central Andes, on the eastern slope of the Andes Mountain range, between the region of Pasco and Junín. It is found at latitudes from 11°18′2″ S to 10°34′6″ S and longitudes from 76°39′14″ W to 75°52′40″ (Datum WGS 84). It is home to the Meseta del Bombón, a gently sloping plateau, with an area of 3017 km^2 and an altitude ranging from 4070 to 4734 masl. Within it are the protected natural areas of Lake Junín, Huallay, and Chacamarca and the second-largest lake in Peru, Lake Chinchaycocha (Figure 1).

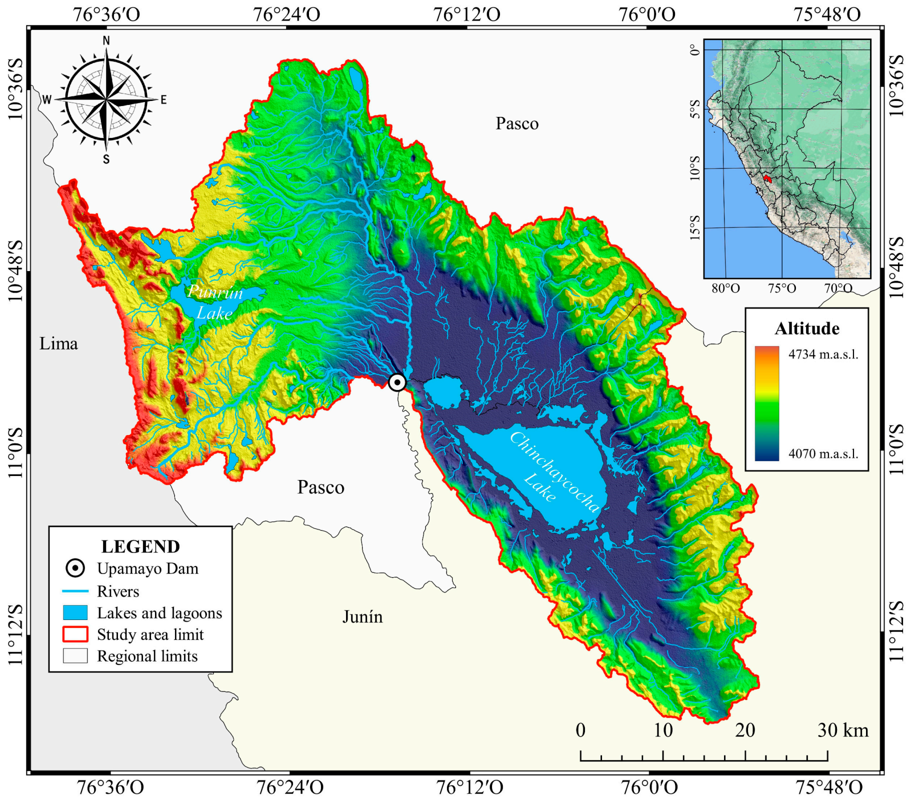

Figure 1. Study area generated from DEM from the Upamayo Dam monitoring station.

The temperature ranges between 0 °C and 14 °C. Precipitation varies between 670 and 1022 mm annually, with two distinct seasons, the rainy season (October–April) and the dry season (May–September). The predominant ecosystem in this area is Puna Húmeda, dominated by high-Andean grasslands such as *Calamagrostis rigida*, *Calamagrostis recta*, *Festuca dolychophylla*, *Stipa ichu*, and *Stipa obtusa*, mainly used in livestock production of sheep, cattle, and alpacas [20,21]. Likewise, in a large part of the territory, wetlands can be found on the shores of Lake Junín with predominant vegetation of *Plantago tubulosa*, *Limosella australis*, *Juncus arcticus*, *Eleocharis albibracteata*, *Deyeuxia recta Kunth*, *Schoenoplectus californicus*, also used in cattle feed and "Champeo" as fuel [22,23].

The delimitation was carried out from the mouth of the tributaries of Lake Chinchaycocha and other small tributaries that converge in the area called "Presa Upamayo" (Lat. 10°55′25″ S; Long. 76°16′43″ W). For this, the procedures for delimiting hydrographic basins were used, using the tools present in the QGIS 3.18.3 software of "Hydrology Terrain Analysis". Inputs for delimitation were used as a basis for the exact location of the mouth and the digital elevation model (DEM) of 30 m resolution, from the ASTER (Advanced Spaceborne Thermal Emission and Reflection Radiometer) of the GDEM 003 (Global Digital Elevation Model version 3). Available at: https://asterweb.jpl.nasa.gov/gdem.asp (accessed 28 March 2023).

2.2. Data Collection

Surface reflectance images with a resolution of 30 m, generated every 16 days by the Landsat 5 TM, 7 ETM, and 8 OLI satellites, were used. Through the median of each pixel, the visual quality of the annual images was improved between 1985 and 2022, during the dry season (April–October), as these are the months with the slightest presence of clouds. All the mentioned filters were executed within the Google Earth Engine (GEE) platform [24].

2.3. Spatial Coverage Analysis

To analyze land-cover change, the collection of Landsat images was harmonized using coefficients calculated by Roy et al. [25], with the OLI reflectance transform method proposed by Vogeler et al. [26]. Supervised classification was applied using the random forest (RF) algorithm combined with a field land-cover data set, using a validated model for high-Andean vegetation developed by Pizarro et al. [8] based on multispectral Landsat data and ALOS PALSAR DEM [27] topographic-derived indices.

To generate training data sets for land-cover classes, we used primary data for vegetation land-cover types and completed with other reference sources such as the 2015 national vegetation map [28] (geliturbated areas, glaciers, water, and bare soil classes), Google Earth imagery (pan-sharpened QuickBird, GeoEye, and WorldView-2 imagery), and visual interpretation.

Training samples were generated from a total of 11,057 pixels (1000 for each class, except glacier with 57 pixels) available (85% from field data, and 15% from Google Earth imagery and the 2015 national vegetation map) and the samples were split into a validation data set in 30/70% proportion by a stratified random sampling method for each cover class to ensure independence between the training and validation data.

The accuracy of the classifier was evaluated with the overall accuracy (OA), kappa coefficient (K), producer accuracy (PA), and user accuracy (UA), where K indicates the degree of agreement between the ground-truth data and the predicted values, while the PA measures how well a pixel has been classified and includes the error of omission (the proportion of observed features on the ground that are erroneously excluded from a class). The UA measures the reliability of the map, informing how well the map represents what is on the ground and it includes the error of commission which refers to pixels erroneously included in a class [29]. The RF classifier generated allowed us to generate past land-cover layers for the defined period, based on the annual historical stacked imagery, for the study area.

The characteristics of each cover type are described in Table 1. They were considered separately for the analysis by types of plant covers and covers considered as a change factor (f). Plant covers are mainly constituted by plant communities of different species that coexist in association with a specific habitat with its particularities (e.g., presence of water and different slopes, among others). While the coverage considered as a change factor (f) is coverage that was altered by anthropogenic activities. In other coverages, spaces that are not part of the analysis of this study were considered, such as lakes, glaciers, and periglaciers.

Table 1. Characteristics of the coverage found in the study area [30].

Classes	Coverage Features
Wetland	Hydrophytic wetland grasses are found in places where there is water upwelling and maintain plant communities composed of cushion-shaped grasses and sedges, with botanical families dominated by *Cyperaceae* and *Juncaceae*, e.g., *Oxychloe andina*, *Distichia muscoids.*
Cattail	Swampy areas are composed mainly of species of the Juncaceae family represented by *Scirpus californicus var*, cattails, and *Juncus articus var. Andicola*, in very dense formations, over seasonal waters.
Bulrush	It is considered a species of the *Juncaceae* family and cattail intermediate growing like *Typha* spp. and *Scirpus* spp. They are found in the presence of permanent water.
Tall grass	Areas composed of tall perennial grasses up to 1 m high, such as the species *Festuca*, *Poa*, *Stipa*, and *Calamagrostis*, with a herbaceous stratum of the genera *Werneria*, *Hypochaeris (Asteraceae)*, and *Geranium (Geraniaceae)*.
Puna grass	Areas dominated by dwarf herbaceous, pink, and cushion plants, growing in areas of moderate water content, with botanical genera of *Cinnagrostis*, *Aciachne (Poaceae)*, *Baccharis*, *Werneria*, *Perezia (Asteraceae)*, and *Opuntia (Cactaceae)*.
Geliturbated areas	Consisting mainly of protruding rocks and remnants of vegetation made up mainly of tall grass and puna grass.
Bare ground (f)	Permanent bare soils without vegetation development.
Agricultural area (f)	Areas of permanent and seasonal cultivation, livestock grazing areas, or crop rangeland.
Urban area (f)	Urban areas, paved and motorized roads, permanent bare soils, river edge gravel, mining activity (mine tailings, open-pit mine, earth movement, non-metallic mining).

The final map was generated considering the median of the pixel values of all the layers generated through supervised classification between 1985 and 2022. Through this process, it was possible to determine the predominance of the various coverages for each pixel and the distribution of the percentage of area occupied by different types of vegetation cover and other categories.

2.4. Vegetation Degradation Analysis

The interannual trend of the atmospheric resistant vegetation index (ARVI) was used to analyze vegetation degradation. Its relationship with biophysical processes, such as productivity and photosynthetic activity [15,31], allows for obtaining more exact approximations in monitoring the health and density of vegetation in Andean ecosystems. This is made up of the following equation:

$$ARVI = \frac{(NIR - 2 * Red + Blue)}{(NIR + 2 * Red + Blue)} \tag{1}$$

where *NIR* corresponds to the near-infrared band (0.85–0.88 μm), *Red* to the Red band (0.64–0.67 μm), and *Blue* to the Blue band (0.45–0.51 μm) of the electromagnetic spectrum [17].

Subsequently, the non-parametric Mann–Kendall test (S) per pixel was applied to the trend of the ARVI to detect changes in the time series [32]. This test offers advantages due to its low sensitivity to outliers, focusing on the ranges of values, but not on the values themselves. Additionally, this test is suitable for small samples [33]. Therefore, its application is favorable due to the characteristics of the data and the advantages it offers [34]. The equation is calculated as the Mann–Kendall correlation coefficient (S), and is configured as follows:

$$S = \sum_{i=1}^{n-1} \sum_{j=i+1}^{n} sign(x_i - x_j) \quad (2)$$

where n is the number of data points; x_i and x_j are the data values in time series i and j when $j > i$. The sign $(x_i - x_j)$ is interpreted according to the sign as follows:

$$sign(x_i - x_j) = \begin{cases} +1 \ if \ x_i - x_j < 0 \\ 0 \ if \ x_i - x_j = 0 \\ -1 \ if \ x_i - x_j > 0 \end{cases} \quad (3)$$

The variance is calculated as follows:

$$VAR(S) = \frac{n(n-1)(2n-5) - \sum_{i=1}^{m} t_i(t_i - 1)(2t_i + 5)}{18} \quad (4)$$

where n is the number of data points, m is the number of linked groups, and t_i denotes the number of extension links i. This is used to evaluate the dispersion of the data.

What is described is input to calculate the Z-score to evaluate the significance as follows:

$$Z = \begin{cases} \frac{S-1}{\sqrt{VAR(S)}}, \ if \ S > 0 \\ 0, \ if \ S = 0 \\ \frac{S+1}{\sqrt{VAR(S)}}, \ if \ S < 0 \end{cases} \quad (5)$$

Z-scores indicate an increasing or decreasing trend of the ARVI, respectively, and a Z-score equal to 0 shows no trend. Comparison between Z and the standard normal variable at the desired significance level α allows for testing the significance of the trend. In this study, a significance level of 5% and 1% was selected, which is the same as $p < 0.05$ and $p < 0.01$, which means that, for example, if $|Z| > 1.96$, the null hypothesis that there is no trend would be rejected. The evaluated trend will be considered slight when the significance is higher than $p < 0.05$ and when the trend is significant, it will be when the significance level exceeds $p < 0.01$. From this analysis, increases, whether slight or significant, will be considered a sign of development or recovery of vegetation, while reduction, whether slight or significant, will be interpreted as a loss or degradation of vegetation.

2.5. Analysis of Data

To carry out a comprehensive analysis, two types of data were collected for each study year: (i) data covering all coverage categories in the study area and (ii) data limited to the coverages affected by vegetation degradation. For both data sets, the following procedures were carried out: (i) To identify the predominance of coverage in each pixel, a consolidated layer was generated by calculating the median from the supervised classification results of all the years analyzed. (ii) The number of pixels corresponding to each coverage was quantified using the QGIS software "report of unique values" tool. These data gave rise to time series, in which the existence of trends and their significance were evaluated by applying the Mann–Kendall model, using a 95% confidence level. (iii) In addition, the means of the areas corresponding to each coverage category were determined and the coefficient of variation was calculated to identify which of them had the most significant variability over time. (iv) Finally, a Spearman correlation analysis was conducted to observe possible substitutions or replacements between the different coverage categories. This analysis was complemented with a graphical representation through a Sankey diagram, which made it possible to visualize the flow of coverage change throughout 1985, 2005, and 2022. MS Excel 2019, R Studio version 4.3.1, and Statgraphics Centurion 19 software were used for this analysis.

3. Results

3.1. Supervised Classification of Total Vegetation Cover

Chinchaycocha is the center, which in its central part contains hydrophilic vegetation, which includes wetlands (9.0%), cattails (3.7%), and bulrush (4.0%). The transition zone is mainly dominated by Andean agriculture (16.4%) and is home to most urban areas (2.1%). In the peripheral part, which extends from the transition part, most of the grass vegetation (21.2%), tall grass (17.7%), and the inclusion of geliturbated areas (13.6%) prevail. Lakes, bare soil, glaciers, and periglaciers constituted 12.3%, with lakes having the most extensive area (8.5%) when considered against other covers (Figure 2). This analysis, based on the median pixel values, provides a more accurate and detailed understanding of the coverage distribution over the period examined.

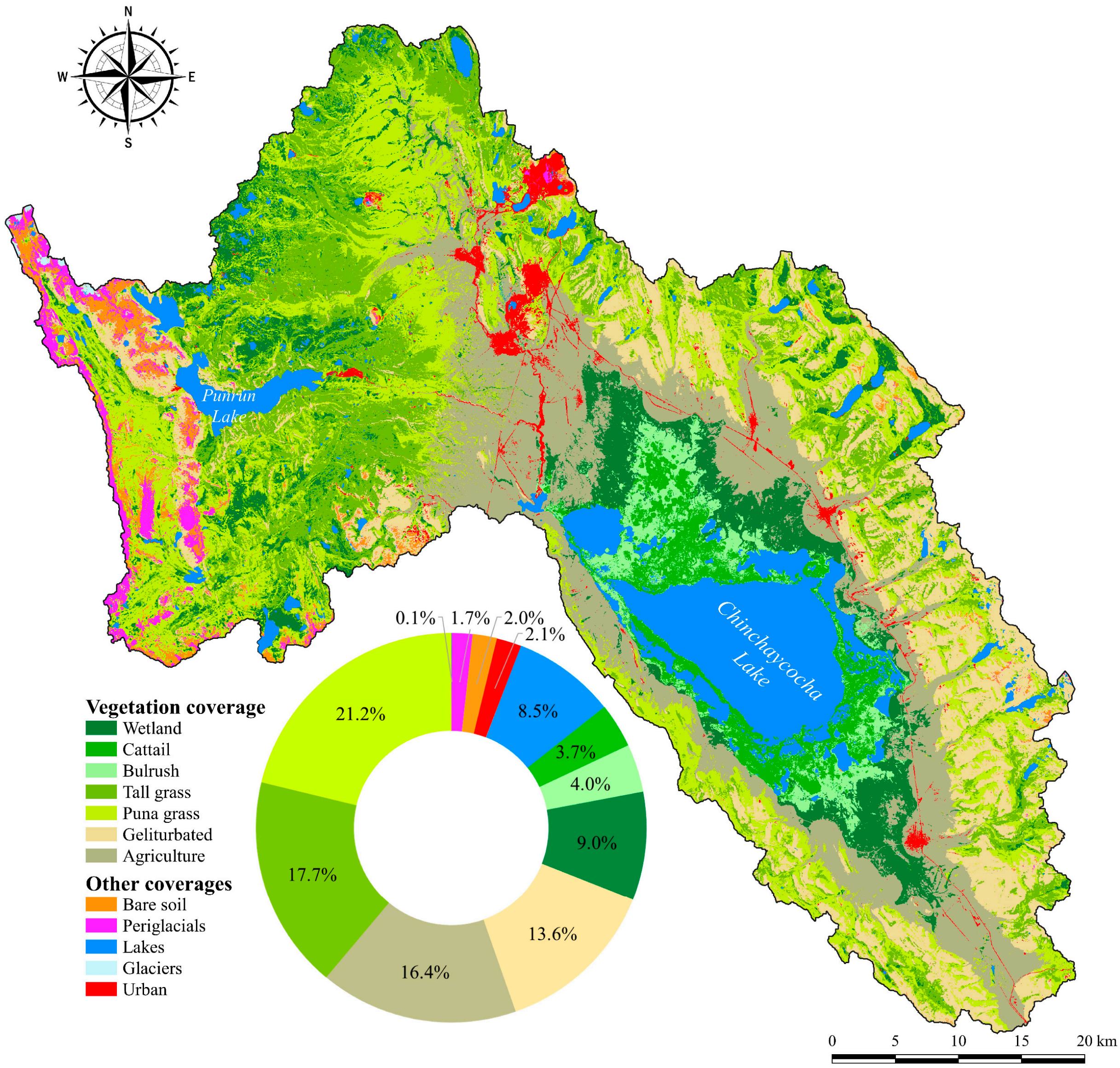

Figure 2. Vegetation cover map of the Bombón Plateau, Peru, based on the median of the supervised classification and proportion to the total in the period 1985–2022.

3.2. Analysis of the Distribution of Degraded Vegetation Cover

The analysis of vegetation cover degradation through the trend of the ARVI reveals that 13.4% of the total cover is degraded, with 6.2% showing significant degradation ($p < 0.01$). Likewise, 12.5% of the vegetation has improved significantly and the most significant proportion of the area (74.2%) is stable (see Figure 3). Vegetation degradation does not have a defined spatial distribution pattern (more detail in Figure 4). A specific separation can be visualized in places classified as urban areas. These are mainly related to places where mining activity occurs, located mainly on the northern side of the study area where there was earth movement and, therefore, urban growth due to the establishment of people related to mining activity. These places are adjacent to the mining city of Cerro de Pasco and nearby cities around Lake Chinchaycocha, such as Carhumayo and Junín.

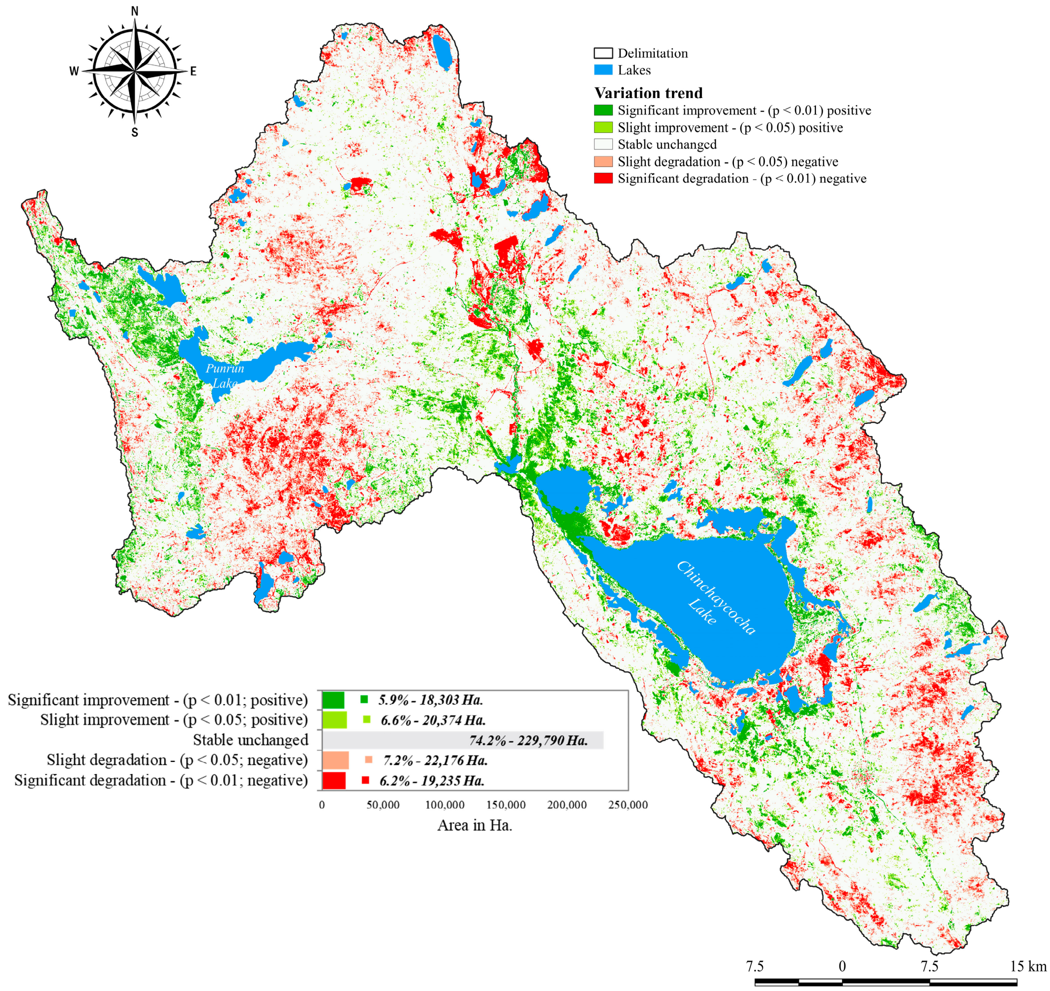

Figure 3. Map of significant ARVI Mann–Kendall trends for the period 1985 to 2022 of the Bombón Plateau, Junín, Peru.

Figure 4 shows the percentage of degraded vegetation covers (DVCs). The count corresponds to the percentage degraded concerning the area occupied by each coverage. The DVC with the most remarkable presence of degraded areas is bulrush (21%) and 13% of significant degradation (p < 0.01), which is located mainly in the near interior part of Lake Chinchaycocha. The following most degraded coverage is tall grass with 18%. This is located mainly between the study area's intermediate and periphery parts in spaces with higher slopes. Cattail, adjacent to Lake Chinchaycocha, represents 16% of the degraded area, and 14% of the wetlands are also degraded. In a smaller proportion, puna grass accounts for 13% and geliturbated areas for 10% of the space degraded (see detail in Figure 4a). Considering the size of each cover within the study area, the most affected areas would be the tall grass, puna grass, and wetlands with 29, 23, and 12% of the total degraded vegetation (see Figure 4b).

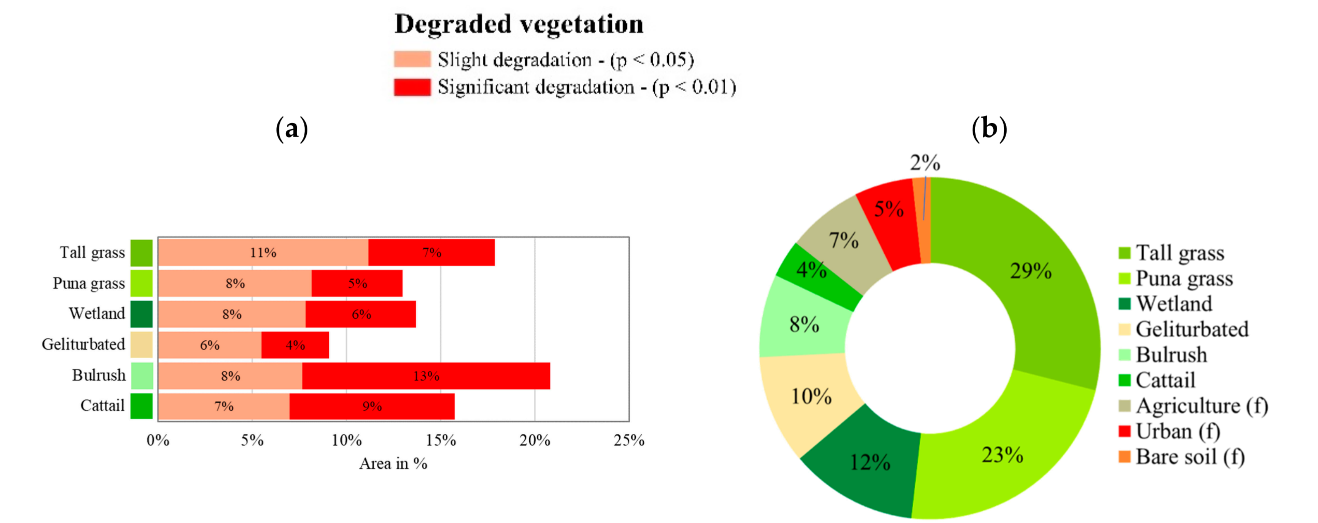

Figure 4. Quantification diagram proportion of degraded vegetation cover. (**a**) The proportion of degraded vegetation covers the area occupied by each cover. Areas with mild degradation in pink ($p < 0.05$) and areas with significant degradation in red ($p < 0.01$). (**b**) The total proportion of degraded vegetation covers.

3.3. Temporal Analysis of Degraded Vegetation Cover

Figure 5 shows the interannual changes in the different vegetation cover types and degraded areas. The years 1991, 1992, and 2002 were excluded due to significant outlier errors. This decision allowed us to carry out a trend analysis over time for each type of cover using the Mann–Kendall trend test, both for the total vegetation covers (TVCs) and degraded vegetation covers (DVCs).

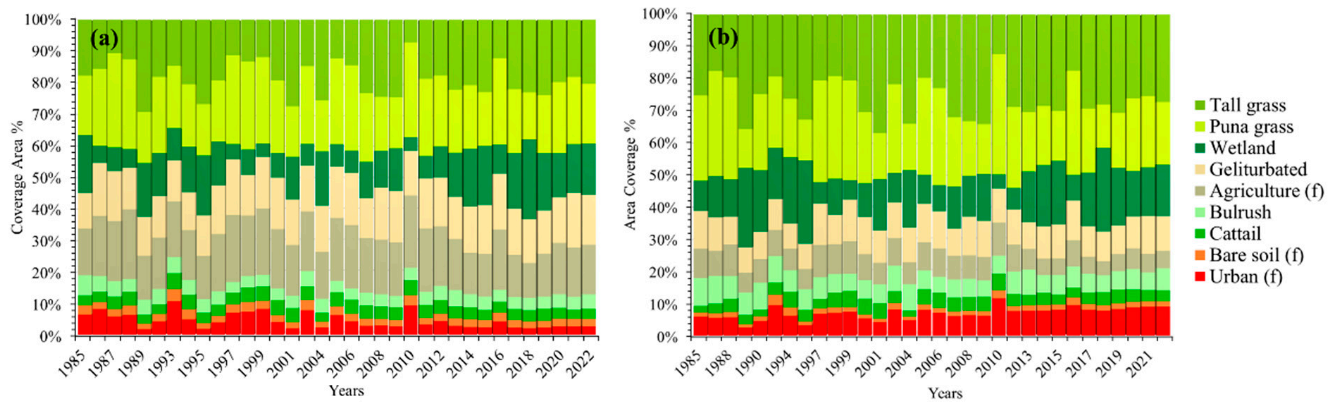

Figure 5. Temporal analysis of the area expressed in percentages in the period 1985–2022 of (**a**) the annual total vegetation cover (TVC) and (**b**) the degraded vegetation cover (DVC).

When examining the TVCs, it is observed that none of the coverages show a significant tendency to decrease or increase ($p > 0.05$; Figure 5a and Table 2). However, it is essential to highlight that bulrush slightly decreased throughout the evaluation period. Additionally, it is observed that some coverage experiences significant increases in specific years, followed by returns to areas like the first years. For example, the coverage of cattails reached maximum areas in 2010, while wetlands experienced a considerable reduction in their coverage, and then recovered. Finally, there has been a slight increase in the coverage of tall grass in recent years.

Table 2. Mean of the occupied area, coefficient of variation (CV %), and Mann–Kendall significance of all the years evaluated (1985–2022) of the vegetal covers and covers considered factors of change.

Coverage	TVC			DVC		
	Mean Area Ha	CV %	Significance Mann–Kendall	Mean Area Ha	CV %	Significance Mann–Kendall
Wetland	32,888.3	45.0	ns	5547.9	39.4	ns
Cattail	10,754.2	23.7	ns	1483.9	23.1	ns
Bulrush	11,927.1	18.8	ns	2594.7	19.3	** (−)
Tall grass	50,600.6	30.8	ns	10,098.7	25.1	ns
Puna grass	61,002.4	20.7	ns	9068.5	32.0	ns
Geliturbated areas	40,629.3	12.2	ns	4023.7	14.8	ns
Bare ground (f)	7046.0	24.5	ns	661.5	29.1	ns
Agricultural area (f)	47,372.8	16.9	ns	2913.6	23.1	** (−)
Urban area (f)	14,763.1	81.8	ns	2821.4	31.8	** (+)

The initials ns mean non-significant trend. The symbol ** expresses significance at a confidence level of 99% or $p < 0.01$. The sign (−) indicates a negative trend. The sign (+) indicates a positive trend.

Regarding the analysis of the DVCs (Figure 5b), it is identified that bulrush shows a tendency to decrease from the years 2009 and 2010, with a significant negative trend according to the Mann–Kendall test ($p > 0.05$). On the other hand, the coverage considered as factors of change, such as the urban area, show a positive trend ($p > 0.01$). In contrast, the coverage associated with agriculture presents a significant tendency to decrease, starting in 2010 ($p > 0.01$; see details in Table 2).

Table 2 provides a detailed analysis of the average area occupied by the total vegetable covers (TVCs) and degraded vegetative covers (DVCs), together with the coefficient of variation (CV %) and the results of the Mann–Kendall trend analysis with a minimum confidence level of 95%. The TVCs that occupy the most extensive areas are puna grass and tall grass, with an intermediate variability of 20.7% and 30.8%, respectively. On the other hand, the TVCs that exhibit more significant variability are the urban areas (81.8%) and wetlands (45.0%). This is complemented by the spatial analysis of CV % of the TVCs in Figure 6a where indeed wetlands, followed by tall grass, are the most variable over time. In terms of trend, none of the TVCs show a significant trend according to the Mann–Kendall test.

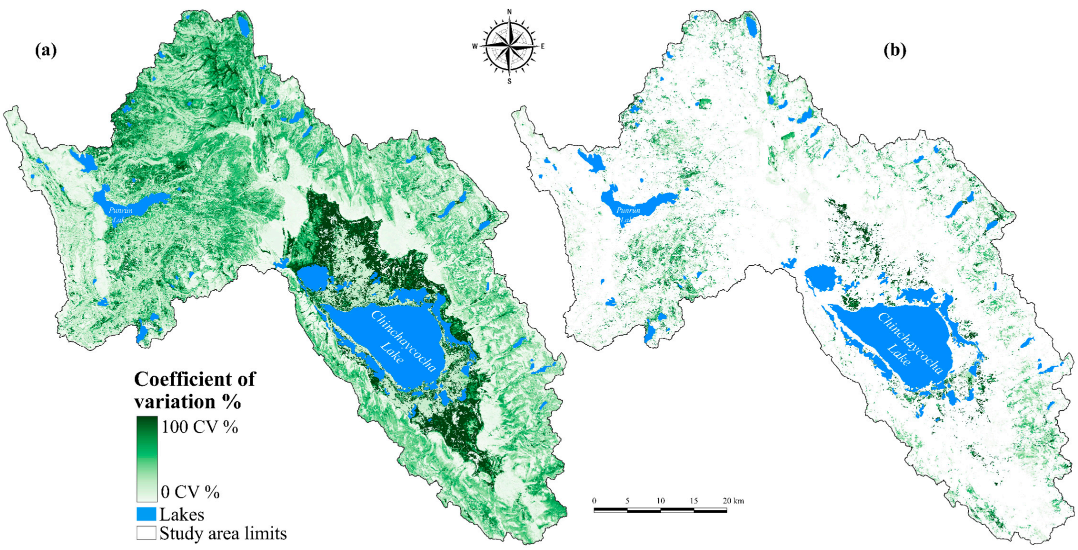

Figure 6. Spatial analysis map of coefficient of variation expressed in % from the annual supervised classification of (**a**) total vegetation cover (TVC) and (**b**) degraded vegetation cover (DVC).

In the case of the DVCs, Table 2 details that tall grass and puna grass are those that occupy the most extensive areas, with variability of 25.1% and 32.0%, respectively. The DVCs that show the most extensive variability are wetlands (39.4%), followed by the urban areas (31.8%), also shown in Figure 6b. The DVCs that show a significant negative trend are bulrush and the agricultural areas, while those that show a significant positive trend are the urban areas ($p < 0.01$).

3.4. Plant Replacement Flow

The Sankey diagram shows the flow or replacement of coverage between 1985, 2005, and 2022. This analysis also evaluates coverage as a change factor (f). In the TVC diagram (Figure 7a), the puna grasslands (1985) initially have the most prominent area, being replaced by puna grass (2005). Similarly, tall grass (2005) returns to its initial state starting with puna grass (2022). Likewise, puna grass receives a significant flow from tall grass (2005), which returns to tall grass (2022). From this approach, these covers complete a "cyclical substitution", that is, the degraded tall grass is replaced mainly by puna grass and then recovers its initial condition. Wetlands, for their part, are replaced by tall grass, grass, and agricultural areas in a more significant proportion, and on the contrary, their recovery is from these same coverages (2022). Furthermore, it replaces cattails and bulrush (2005) but to a lesser extent. Therefore, the increase in agricultural areas impacts the reduction in wetlands and grass. The latter is explained by the proliferation of wetlands in the external part of the study area, and they are close to tall grass and puna grass. In the intermediate part of the study area, its relationship with the agricultural area means that it influences it (see distribution in Figure 2).

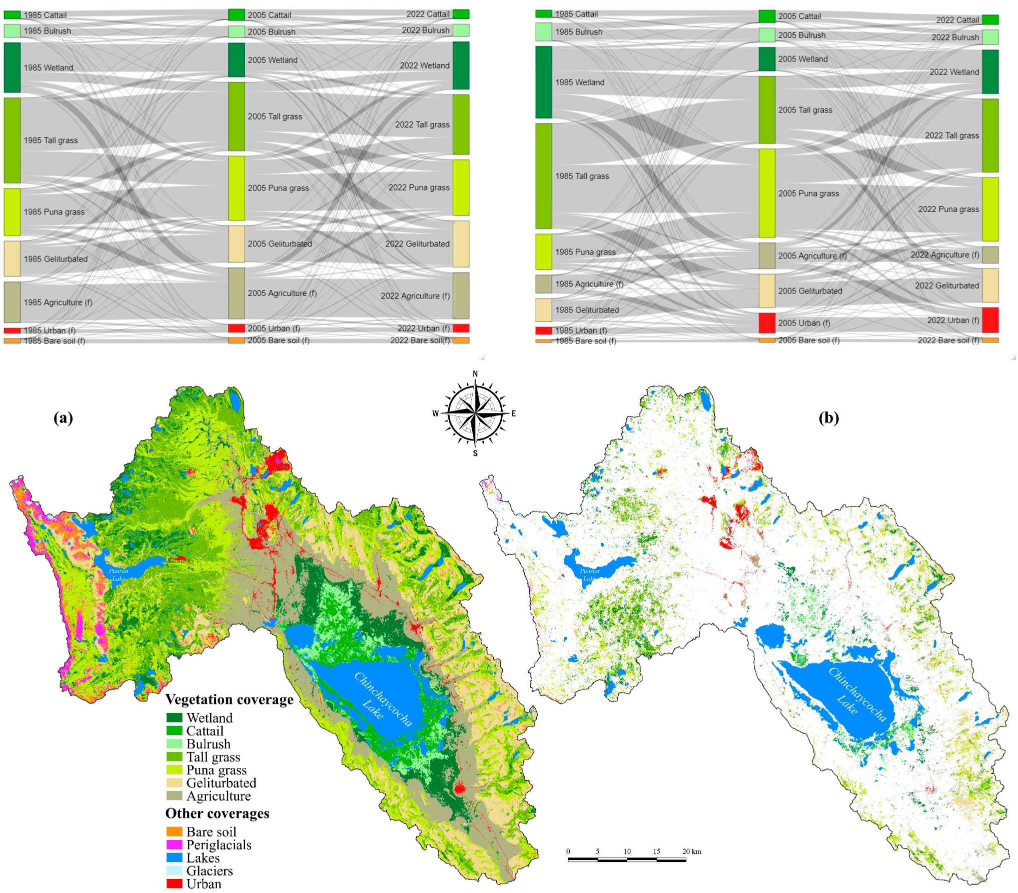

Figure 7. Sankey diagram of the flow for the replacement of coverage for the years 1985–2005–2022, of (**a**) the total vegetation cover and (**b**) the degraded vegetation cover. The map images help determine whether you are talking about TVC or DVC.

Something similar is shown in the DVCs (Figure 7b). Tall grass (1985) is replaced by puna grass and geliturbated areas (2005) and its recovery is from these same coverages (2022). Puna grass increases considerably from tall grass and wetlands (2005) to return to its original area, returning the flow to the same coverage (2022). Wetlands are replaced by tall grass, puna grass, agricultural areas, and bulrush (2005). However, this does not return to its initial state, being one of the few areas recovered from the same coverage (2022). Geliturbated vegetation areas increase (2005) from grasslands and make an exchange toward puna grass (2022). The flow between bulrush and cattails is constant with a slight exchange with wetlands.

3.5. Spearman Correlation Analysis for Vegetation Cover Replacement Evaluation

In Figure 8, to focus on the most relevant aspects of the analysis, the relationship between the different vegetation covers over the years was investigated through a Spearman correlation matrix. This matrix involves both the total vegetation cover (TVC; Figure 8a) and degraded vegetation cover (DVC; Figure 8b). The critical consideration here is a correlation coefficient greater than 0.6 or less than −0.6, with a significance greater than 99.99% ($p \leq 0.001$). Finding a significant positive correlation may indicate an association that goes beyond chance, suggesting dependence or complementarity. On the other hand, a significant negative correlation may signal competition or substitution between hedges.

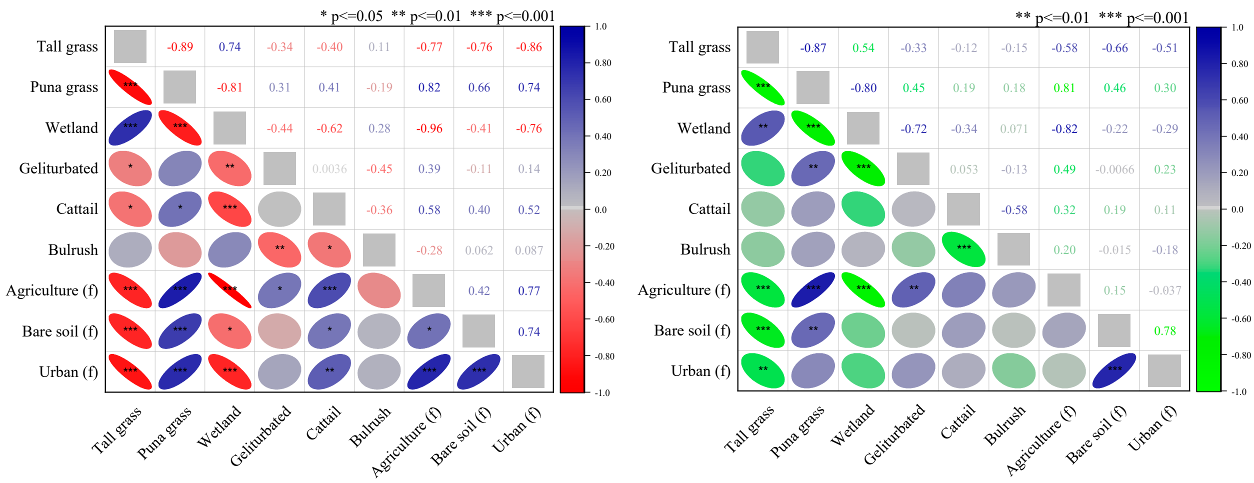

(**a**) (**b**)

Figure 8. Spearman correlation analysis between the covers of all years, of the (**a**) total vegetation covers (TVCs) and (**b**) the degraded vegetation covers.

We observe in the TVC correlation matrix (Figure 8a) that tall grass shows a negative correlation with most of the covers, except for wetlands and bulrush. Similarly, wetlands have negative correlations with almost all coverage, except tall grasses and bulrush. This information highlights that tall grass and wetlands tend to be replaced by puna grass and change factors (f) such as agricultural area, urban area, and bare soil. On the contrary, puna grass shows a positive and significant correlation with most plant covers, except wetlands, tall grass, and bulrush. Similarly, in the Spearman correlation matrix of the DVCs (Figure 8b), both tall grass and wetlands present a positive and significant correlation with puna grass. This can be interpreted as a relationship in which puna grass replaces these degraded covers to a greater extent after having suffered degradation due to changes in agricultural areas, bare soil, and urban areas, with which they also show a significant positive correlation. On the other hand, the correlation between geliturbated areas and wetlands lacks causality, since no clear spatial connection is identified. Finally, puna grass increases significantly when the change factors experience an increase, for example, the agricultural area.

4. Discussion

The distribution of vegetation cover around Lake Chinchaycocha reveals a defined segmentation that ranges from the humid central area to peripheral spaces dominated by puna and geliturbada vegetation. This segmentation is a testament to the diverse ecological niches present in the region, each with its unique set of flora adapted to the specific conditions. Although specific to the lake and its surroundings, these ecological and landscape characteristics find parallels in other mountainous and highland regions. It is worth noting that similar ecological patterns, influenced by both natural and human-induced factors, have been observed in other high-altitude regions around the world. Human activities, such as changes in land use and agricultural practices, also play a crucial role in shaping vegetation cover. The interplay between natural conditions and human intervention creates a dynamic landscape that is constantly evolving. This study identified that the transition or "intermediate" zone is mainly dominated by the agricultural area (16.4%), which suggests intense agricultural activity near the lake. Studies in the Chinese Loess Plateau have shown that agricultural modernization and land-use changes can lead to soil erosion and vegetation degradation [35]. Although erosion is not mentioned explicitly in our results, it is a factor to consider given the significant presence of agricultural areas. The potential for soil erosion, especially in areas with steep slopes, can have cascading effects on the local ecosystem, affecting water quality, habitat availability, and overall biodiversity.

The total degraded area was determined to correspond to 13.4% of the areas with vegetation cover. This is less than estimated (60%) and is mainly caused by poor management, burning, overgrazing, and climate change [36]. These differences are because the analysis takes the spaces that have remained in a state of progressive degradation for almost four decades and have not returned to their initial state. The current analysis takes recently degraded spaces that are possibly recovered or are in a plant succession cycle process [37–39]. Understanding the reasons behind these differences is crucial. It could be indicative of irreversible damage to certain vegetation types or a shift in the ecological balance of the region. This vegetation degradation is generated mainly by human activities such as changes in land use, increased human population, and the intensification of activities such as agriculture, livestock, and mining. Likewise, the effects of climate change and variation in precipitation patterns and atypical temperature ranges influence vegetation's spatial and temporal dynamics, added to the intrinsic limitations of ecological floors above 4000 masl [40].

Climate change and human activities affect vegetation trends. Research in the Qinghai–Tibet Plateau has shown that urban expansion can negatively affect vegetation change [41]. In the context of Lake Chinchaycocha, where a presence of the urban area (2.1%) was identified in the intermediate zone, it is vital to consider how urban expansion could influence future vegetation trends. Urban areas, with their concrete structures and heat islands, can modify local micro-climates, potentially affecting the surrounding vegetation. The temporal behavior of vegetation covers and their relationship with human activities, such as urbanization and mining, is a topic of growing interest in the scientific literature. In the context of our study, the trend of degraded vegetation covers (DVCs) and its interaction with urban and agricultural areas provides valuable insight into the ecological dynamics in the region. The positive trend observed in urban areas ($p > 0.01$) is consistent with the existing literature suggesting that activities associated with urban areas, especially mining, have significant negative impacts on vegetation cover and land use [42]. In particular, studies in Nigeria and China have highlighted the extensive damage caused by mining, including sand mining, in peri-urban and urban areas, respectively [43,44]. These findings support the idea that mining activities contribute to land degradation in urban areas, which could explain the trends observed in our study.

The degradation pattern of the high-Andean vegetation cover is also promoted by factors such as water deficit due to the absence of precipitation, and temperature variations due to climate change [45]. Likewise, topography plays an important role. Areas with gentle slopes are conducive to developing puna agriculture and grass [46], due to the accumulation of organic matter used in producing Andean crops and livestock [47]. On the other hand, the steep slope acts as a driver for vegetal covers such as tall grass. The prevalence of these covers in these conditions is primarily due to their ability to resist the effects of wind and their adaptation to environments with limited water availability [48]. This agrees with what was found in a study in an Andean micro-basin in Peru [49], where it mentions that the floristic diversity and biodiversity of plant species varies according to the altitude and slope. The adaptability of these vegetation types is a testament to the resilience of nature, but it also underscores the importance of preserving these unique ecosystems that have evolved over millennia.

On the other hand, the significant tendency of a decrease in the coverage composed of agriculture ($p > 0.01$) from 2010 onward could be related to urban expansion and mining, which often displace agricultural areas. The change in land use for agriculture is the greatest threat to these ecosystems, leading to biodiversity loss, andslow plant revegetation and productivity. For example, in the grassland region of the Río de la Plata, the area covered by grasslands decreased between 1985 and 1989 and 2002 and 2004, with an increase in the area of annual crops [50]. Expansion of crop production to high-altitude native grasslands in the Peruvian High Andes is also occurring, converting grasslands to annual cash crop systems [51].

The most extensive areas of TVC, such as puna grass and tall grass, are consistent with the characteristics of the Andean grasslands, which are predominantly covered by species of grasses and herbaceous plants adapted to altitudes between 3500 and 5000 masl., forming areas of grasslands essential in providing ecosystem services fundamental for human life and biodiversity [52]. On the other hand, the high variability observed in urban areas and wetlands is aligned with studies that have identified significant variability in vegetation cover in urban areas and wetlands [53]. In particular, wetlands, with their diversity of aquatic and semi-aquatic species, are susceptible to prolonged droughts, seasonality, and soil characteristics, which can influence the germination and recovery of vegetation [54].

The degradation associated with urban areas and mining activities, especially near cities and lakes, has been widely studied in the literature [55,56]. These activities have been shown to have significant negative impacts on the environment, particularly on vegetation cover and land use [57]. In particular, wetlands are highly susceptible to invasive species, which can lead to changes in the structure of their green food webs and the formation of monocrops [58]. Furthermore, wetlands are prone to degradation and succession processes, resulting in a gradient of degradation from typical wetlands to wet grasslands, typical high-Andean grasslands, and grasslands [59]. Likewise, plant covers such as wetlands, bulrush, and cattail depend on the presence of water and present significant degradation. This shows that these vegetation types are susceptible to environmental or management changes in biological richness and productivity [7,60]. Furthermore, they can undergo substantial changes over time, and not all areas necessarily return to their original state after degradation [61]. Under this, our study reveals that wetlands are replaced by tall grass, puna grass, and agricultural areas. With a minimum recovery rate, the degradation can significantly alter the vegetal composition, plant diversity, primary productivity, and ground fertility. In this context, tall grass and puna grass are indicators of these dynamics, especially with agricultural expansion [62].

Although the present study does not specifically focus on restoration measures, it is necessary to consider the stability of the site and its relationship with changes in vegetation. The ecological impacts of restoration interventions on soils can directly influence plant community composition [61]. In areas such as the study area with a predominance of livestock activity, it is highlighted that the intensity of grazing is a determining factor in the restoration of degraded grasslands [63]. Although not directly mentioned in the results, it is essential to consider how grazing practices in the region may be influencing the observed substitutions in vegetation covers.

In addition, factors such as climate change and nitrogen deposition can also influence the dynamics of the vegetation cover types suitable for grazing [64,65]. These factors, and anthropogenic activities such as agricultural expansion, may contribute to the dynamics observed in the study area. The Spearman correlation matrix, presented in Figure 7, provides a detailed view of the interactions between vegetation covers throughout the years considered in this study. Although specific to the study area, these interactions are reflected in previous research, where it has been identified that total vegetation covers, such as tall grass and wetlands, tend to be replaced by puna grass and anthropogenic areas such as agricultural and urban areas [66]. This trend is reflected in our study, where tall grass and wetlands show negative correlations with most covers, primarily replaced by puna grass and areas considered a change factor.

Although it is true, the approach used may contain some biases, both in the supervised classification and in evaluating the vegetation trend through the ARVI. However, this study offers an outstanding contribution to the evaluation of vegetation ecosystem degradation. Several studies are recognized that carried out supervised classification and determined the dynamics of coverage in a generic way [67–70]. Unlike other studies, our study showcases a supervised classification tailored to the characteristics of the Andean ecosystems, offering a more specific estimation of their temporal dynamics. This specificity sets our study apart, emphasizing its uniqueness in exploring the dynamics of high-Andean Peruvian vegetation. However, there are some limitations to consider. The supervised classification approach, while robust, may contain biases that could influence the results. Additionally, the ARVI, though widely used, has its own set of limitations in capturing the full spectrum of vegetation dynamics. Future research could employ a combination of different vegetation indices and incorporate ground-truthing methods to validate remote sensing results.

5. Conclusions

The present study provides a spatial and temporal vision of the changes between vegetation covers and their degradation, and the dynamics of replacement and ecological succession, analyzed based on remote sensing products over nearly four decades. Our main findings indicate that the total degraded area corresponds to 13.4% of the studied space, with the most impacted vegetation covers being bulrush, cattails, and tall grass. The coverage with the most significant increase is puna grass and the change factor such as urban areas. Specifically, bulrush was degraded by 21%, tall grass by 18%, cattails by 16%, wetlands by 14%, and puna grass by 13%. It was observed that puna grass replaced most degraded vegetation and changed factors such as agricultural areas, urban areas, and bare soil. These findings demonstrate the degree of vulnerability of the vegetation and the information generated is presented as a vital tool to identify priority conservation and management areas based on the interactions between the extension of the vegetation cover type and the patterns of vegetation degradation due to the effect of human activities over time.

These findings have notable implications for understanding the dynamics of change in plant communities in high-Andean Peruvian areas. This is because fundamental and useful information is presented for the formulation of adaptive management plans, in terms of sustainable use and management, as well as for the conservation of vegetation in these vulnerable ecosystems. This study determined that a significant part of the vegetation degradation is related to anthropogenic activities. However, the possibility that combined environmental factors have influenced these degradation events is also recognized, through variability and anomalies in precipitation, temperature, and humidity due to climate change, as well as the influence of the slope and elevation on diversity, and the composition of communities and plant species. Future studies could delve deeper into quantifying the exact influence of each of these factors, providing a more holistic understanding of vegetation change dynamics in high-altitude ecosystems.

Author Contributions: Conceptualization, D.C. and S.P.; methodology, D.C.; software, D.C. and S.P.; validation, R.P. and R.Y.; formal analysis, C.C.; investigation, D.C. and S.P.; writing—original draft preparation, D.C. and C.C.; writing—review and editing, D.C., S.P., R.P., C.C., R.Y. and M.L.G.; visualization, D.C., S.P., R.P., C.C., R.Y. and M.L.G.; supervision, D.C. and C.C. All authors have read and agreed to the published version of the manuscript.

Funding: The APC was funded by the Research Department of the Catholic University of Temuco, Chile, and the vice-rector for research at the Universidad de Huánuco, Peru.

Institutional Review Board Statement: Not applicable.

Informed Consent Statement: Not applicable.

Data Availability Statement: The data presented in this study are available on request from the corresponding author.

Conflicts of Interest: The authors declare no conflict of interest.

Abbreviations

ARVI	Atmosphere resistant vegetation index
NIR	Near-infrared
GEE	Google Earth Engine
GIS	Geographical Information System
CV	Coefficient of variation
TVC	Total vegetation cover
DVC	Degraded vegetation cover
masl	Meters above sea level
Ha	Hectare

References

1. Ochoa-Sánchez, A.E.; Crespo, P.; Carrillo-Rojas, G.; Marín, F.; Célleri, R. Unravelling evapotranspiration controls and components in tropical Andean tussock grasslands. *Hydrol. Process.* **2020**, *34*, 2117–2127. [CrossRef]
2. Iannacone, J.; Alvariño, L. Diversidad de la artropofauna terrestre en la Reserva Nacional de Junín, Perú. *Ecol. Apl.* **2006**, *5*, 171–174. Available online: http://www.scielo.org.pe/scielo.php?script=sci_arttext&pid=S1726-22162006000100023&lng=es&nrm=iso&tlng=pt (accessed on 17 February 2023). [CrossRef]
3. Iannacone, J.; Alvariño, L. Diversidad del zooplancton en la Reserva Nacional de Junín, Perú. *Ecol. Apl.* **2006**, *5*, 175–181. Available online: http://www.scielo.org.pe/scielo.php?script=sci_arttext&pid=S1726-22162006000100024&lng=es&nrm=iso&tlng=es (accessed on 17 February 2023). [CrossRef]
4. Peñaloza, R.; Custodio, M.; Cacciuttolo, C.; Chanamé, F.; Cano, D.; Solorzano, F. Human Health Risk Assessment for Exposure to Heavy Metals via Dietary Intake of Rainbow Trout in the Influence Area of a Smelting Facility Located in Peru. *Toxics* **2023**, *11*, 764. [CrossRef]
5. Dai, H.; Huang, G.; Wang, J.; Zeng, H. VAR-tree model based spatio-temporal characterization and prediction of O3 concentration in China. *Ecotoxicol. Environ. Saf.* **2023**, *257*, 114960. [CrossRef] [PubMed]
6. Dai, H.; Huang, G.; Zeng, H. Multi-objective optimal dispatch strategy for power systems with Spatio-temporal distribution of air pollutants. *Sustain. Cities Soc.* **2023**, *98*, 104801. [CrossRef]
7. Maldonado Fonkén, M.S. An introduction to the bofedales of the Peruvian High Andes. *Mires Peat* **2014**, *15*, 1–13.
8. Pizarro, S.E.; Pricope, N.G.; Vargas-Machuca, D.; Huanca, O.; Ñaupari, J. Mapping Land Cover Types for Highland Andean Ecosystems in Peru Using Google Earth Engine. *Remote Sens.* **2022**, *14*, 1562. [CrossRef]
9. Carpio, L.D.; Taype-Huamán, I. Análisis multitemporal de asociaciones vegetales y cambios de uso del suelo en una localidad altoandina, Puno-Perú. *Uniciencia* **2021**, *35*, 1–19. Available online: https://www.revistas.una.ac.cr/index.php/uniciencia/article/view/14783/21426 (accessed on 28 July 2023). [CrossRef]
10. Mantas, V.; Caro, C. User-Relevant Land Cover Products for Informed Decision-Making in the Complex Terrain of the Peruvian Andes. *Remote Sens.* **2023**, *15*, 3303. [CrossRef]
11. Liu, C.; Huang, H.; Sun, F. A Pixel-Based Vegetation Greenness Trend Analysis over the Russian Tundra with All Available Landsat Data from 1984 to 2018. *Remote Sens.* **2021**, *13*, 4933. [CrossRef]
12. Torres-Batlló, J.; Martí-Cardona, B.; Pillco-Zolá, R. Mapping evapotranspiration, vegetation and precipitation trends in the catchment of the shrinking lake poopo. *Remote Sens.* **2020**, *12*, 73. [CrossRef]
13. Marin, N.A.; Barboza, E.; López, R.S.; Vásquez, H.V.; Fernández, D.G.; Murga, R.E.T.; Briceño, N.B.R.; Oliva-Cruz, M.; Torres, O.A.G.; López, J.O.S.; et al. Spatiotemporal Dynamics of Grasslands Using Landsat Data in Livestock Micro-Watersheds in Amazonas (NW Peru). *Land* **2022**, *11*, 674. [CrossRef]

14. Kombate, A.; Folega, F.; Atakpama, W.; Dourma, M.; Wala, K.; Goïta, K. Characterization of Land-Cover Changes and Forest-Cover Dynamics in Togo between 1985 and 2020 from Landsat Images Using Google Earth Engine. *Land* **2022**, *11*, 1889. [CrossRef]
15. Kaufman, Y.J.; Tanré, D. Atmospherically Resistant Vegetation Index (ARVI) for EOS-MODIS. *IEEE Trans. Geosci. Remote Sens.* **1992**, *30*, 261–270. [CrossRef]
16. Lang, M.; Mahyou, H.; Tychon, B. Estimation of rangeland production in the arid oriental region (Morocco) combining remote sensing vegetation and rainfall indices: Challenges and lessons learned. *Remote Sens.* **2021**, *13*, 2093. [CrossRef]
17. Harmse, C.J.; Gerber, H.; Van Niekerk, A. Evaluating Several Vegetation Indices Derived from Sentinel-2 Imagery for Quantifying Localized Overgrazing in a Semi-Arid Region of South Africa. *Remote Sens.* **2022**, *14*, 1720. [CrossRef]
18. Jiang, F.; Deng, M.; Long, Y.; Sun, H. Spatial Pattern and Dynamic Change of Vegetation Greenness from 2001 to 2020 in Tibet, China. *Front. Plant Sci.* **2022**, *13*, 892625. [CrossRef]
19. Jiang, W.; Yuan, L.; Wang, W.; Cao, R.; Zhang, Y.; Shen, W. Spatio-temporal analysis of vegetation variation in the Yellow River Basin. *Ecol. Indic.* **2015**, *51*, 117–126. [CrossRef]
20. Portillo, V. *Evaluación de Amenazas por Pastoreo al Pastizal del Humedal de la Comunidad Campesina Santa Clara de Chuiroc—Reserva Nacional de Junín, 2018*; Tesis Para Optar el Título Profesional de Ingeniera Ambiental; Universidad Continental: Huancayo, Perú, 2021; Available online: https://repositorio.continental.edu.pe/handle/20.500.12394/9484 (accessed on 27 February 2023).
21. Shoobridge, D. Perfil de Área Natural Protegida Perú Reserva Nacional de Junín. 2006. Available online: https://www.parkswatch.org/parkprofiles/pdf/jnar_spa.pdf (accessed on 12 August 2023).
22. Medrano, R.; Yanqui, R.M.; Chupan Minaya, L.; Vila Balbín, M. Almacenamiento de carbono en especies predominantes de flora en el lago Chinchaycocha. *Apunt. Cienc. Soc.* **2012**, *2*, 110–117. Available online: https://journals.continental.edu.pe/index.php/apuntes/article/view/52 (accessed on 27 February 2023). [CrossRef]
23. Caro, C.; Sánchez, E.; Quinteros, Z.; Castañeda, L. Respuesta De Los Pastizales Altoandinos a La Perturbación Generada Por Extracción Mediante La Actividad De "Champeo" En Los Terrenos De La Comunidad Campesina Villa De Junín, Perú. *Ecol. Apl.* **2014**, *13*, 85. [CrossRef]
24. Gorelick, N.; Hancher, M.; Dixon, M.; Ilyushchenko, S.; Thau, D.; Moore, R. Google Earth Engine: Planetary-scale geospatial analysis for everyone. *Remote Sens. Environ.* **2017**, *202*, 18–27. [CrossRef]
25. Roy, D.P.; Kovalskyy, V.; Zhang, H.K.; Vermote, E.F.; Yan, L.; Kumar, S.S.; Egorov, A. Characterization of Landsat-7 to Landsat-8 reflective wavelength and normalized difference vegetation index continuity. *Remote Sens. Environ.* **2016**, *185*, 57–70.
26. Vogeler, J.C.; Braaten, J.D.; Slesak, R.A.; Falkowski, M.J. Extracting the full value of the Landsat archive: Inter-sensor harmonization for the mapping of Minnesota forest canopy cover (1973–2015). *Remote Sens. Environ.* **2018**, *209*, 363–374. [CrossRef]
27. Rosenqvist, A.; Shimada, M.; Ito, N.; Watanabe, M. ALOS PALSAR: A pathfinder mission for global-scale monitoring of the environment. *IEEE Trans. Geosci. Remote Sens.* **2007**, *45*, 3307–3316. [CrossRef]
28. Ministerio del Ambiente (MINAM). Mapa Nacional de Cobertura Vegetal—Memoria Descriptiva. Lima. 2015. Available online: https://www.gob.pe/institucion/minam/informes-publicaciones/2674-mapa-nacional-de-cobertura-vegetal-memoria-descriptiva (accessed on 23 June 2023).
29. Congalton, R.G. A review of assessing the accuracy of classifications of remotely sensed data. *Remote Sens. Environ.* **1991**, *37*, 35–46. [CrossRef]
30. Mónica, A.; Luis, C.; Cornejo, F.M.; Antuane, C.; Roberto, E.; Rosa, G.; Natalia, L.; Ronald, M.; Berenice, M.; Jhordy, O. *Reserva Nacional de Junín. Un Espejo en Medio de los Andes*; SERNANP: Lima, Peru, 2020; Available online: https://sis.sernanp.gob.pe/ (accessed on 11 September 2023).
31. Huete, A.; Justice, C.; Liu, H. Development of vegetation and soil indices for MODIS-EOS. *Remote Sens. Environ.* **1994**, *49*, 224–234. [CrossRef]
32. Helsel, D.R.; Frans, L.M. Regional Kendall test for trend. *Environ. Sci. Technol.* **2006**, *40*, 4066–4073. [CrossRef]
33. Sun, W.; Song, H.; Yao, X.; Ishidaira, H.; Xu, Z. Changes in Remotely Sensed Vegetation Growth Trend in the Heihe Basin of Arid Northwestern China. *PLoS ONE* **2015**, *10*, e0135376. [CrossRef]
34. Li, Z.; Huffman, T.; McConkey, B.; Townley-Smith, L. Monitoring and modeling spatial and temporal patterns of grassland dynamics using time-series MODIS NDVI with climate and stocking data. *Remote Sens. Environ.* **2013**, *138*, 232–244. [CrossRef]
35. Xin, Z.B.; Xu, J.X.; Zheng, W. Spatiotemporal variations of vegetation cover on the Chinese Loess Plateau (1981-2006): Impacts of climate changes and human activities. *Sci. China Ser. D Earth Sci.* **2008**, *51*, 67–78. [CrossRef]
36. Valverde, H.; Fuentealba, B.; Blas, L.; Oropeza Editado, T. *La Importancia de los Pastizales Altoandinos Peruanos (Folleto)*; Dirección de Investigación en Ecosistemas de Montaña—Instituto Nacional de Investigación en Glaciares y Ecosistemas de Montaña (DIEM-INAIGEM), 2022; Available online: https://repositorio.inaigem.gob.pe/bitstreams/8f8bf505-e241-4af0-91ae-4c9e9033ee15/download#:~:text=Sin%20embargo%2C%20m%C3%A1s%20del%2060,p%C3%A9rdida%20de%20biodiversidad%20y%20desertificaci%C3%B3n4 (accessed on 5 October 2023).
37. Zhou, H.; Zhao, X.; Tang, Y.; Gu, S.; Zhou, L. Alpine grassland degradation and its control in the source region of the Yangtze and Yellow Rivers, China. *Grassl. Sci.* **2005**, *51*, 191–203. [CrossRef]
38. Shen, H.; Dong, S.; DiTommaso, A.; Xiao, J.; Zhi, Y. N deposition may accelerate grassland degradation succession from grasses- and sedges-dominated into forbs-dominated in overgrazed alpine grassland systems on Qinghai-Tibetan Plateau. *Ecol. Indic.* **2021**, *129*, 107898.

39. Briske, D.D.; Briske, D.D.; Illius, A.W.; Anderies, J.M.; Illius, A.W.; Anderies, J.M. *Nonequilibrium Ecology and Resilience Theory*; Springer: Berlin/Heidelberg, Germany, 2017; pp. 197–227. Available online: https://link.springer.com/chapter/10.1007/978-3-319-46709-2_6 (accessed on 19 September 2023).
40. Tovar, C.; Carril, A.F.; Gutiérrez, A.G.; Ahrends, A.; Fita, L.; Zaninelli, P.; Flombaum, P.; Abarzúa, A.M.; Alarcón, D.; Aschero, V.; et al. Understanding climate change impacts on biome and plant distributions in the Andes: Challenges and opportunities. *J. Biogeogr.* **2022**, *49*, 1420–1442. [CrossRef]
41. Chen, J.; Yan, F.; Lu, Q. Spatiotemporal Variation of Vegetation on the Qinghai–Tibet Plateau and the Influence of Climatic Factors and Human Activities on Vegetation Trend (2000–2019). *Remote Sens.* **2020**, *12*, 3150. [CrossRef]
42. Xu, X.; Cai, H.; Sun, D.; Hu, L.; Banson, K.E. Impacts of Mining and Urbanization on the Qin-Ba Mountainous Environment, China. *Sustainability* **2016**, *8*, 488. [CrossRef]
43. Fu, Y.; Zhang, Y. Research on temporal and spatial evolution of land use and landscape pattern in Anshan City based on GEE. *Front. Environ. Sci.* **2022**, *10*, 988346. [CrossRef]
44. Awoyelu, F.E.; Mebo, R.A. Effects of sand mining on peri-urban agriculture in Ife East and Ife Central Local Government Areas, Osun State, Nigeria. *Agro-Science* **2022**, *21*, 101–107. [CrossRef]
45. Carilla, J.; Aráoz, E.; Foguet, J.; Casagranda, E.; Halloy, S.; Grau, A. Hydroclimate and vegetation variability of high Andean ecosystems. *Front. Plant Sci.* **2023**, *13*, 1067096.
46. Madrigal-Martínez, S.; Miralles, I.; García, J.L.; Molina, L.; Lima, P. Land-change dynamics and ecosystem service trends across the central high-Andean Puna. *Sci. Rep.* **2019**, *9*, 9688. Available online: https://www.nature.com/articles/s41598-019-46205-9 (accessed on 12 September 2023).
47. Huaraca-Meza, F.; Custodio, M.; Peñaloza, R.; Alvarado-Ibañez, J.; Paredes, R.; De la Cruz, H.; Arzapalo, L.; Lazarte-Pariona, F. Bacterial diversity in high Andean grassland soils disturbed with Lepidium meyenii crops evaluated by metagenomics. *Braz. J. Biol.* **2021**, *82*, e240184. [CrossRef]
48. de Langre, E. Effects of Wind on Plants. *Annu. Rev. Fluid Mech.* **2008**, *40*, 141–168. [CrossRef]
49. Yaranga, R.M.; Pizarro, S.E.; Cano, D.; Chanamé, F.C.; Orellana, J.A. Composition, Diversity, and Value of Ecological Importance in Andean Grassland Ecosystems according to the Altitudinal Gradient in the Huacracocha Micro-Watershed, Peru. *Annu. Res. Rev. Biol.* **2023**, *38*, 43–56. [CrossRef]
50. Farley, K.A.; Bremer, L.L.; Harden, C.P.; Hartsig, J. Changes in carbon storage under alternative land uses in biodiverse Andean grasslands: Implications for payment for ecosystem services. *Conserv. Lett.* **2013**, *6*, 21–27. [CrossRef]
51. Baldi, G.; Paruelo, J.M. Land-Use and Land Cover Dynamics in South American Temperate Grasslands. *Ecol. Soc.* **2008**, *13*, art6. [CrossRef]
52. Yaranga, R.; Van Vuure, A.; Fuentes, A.; Fuentes, A.; Maraví, K.; Román, M.; Cáceres, D.; Fuentes, C.A. Andean Grassland Species: Net Aerial Primary Productivity, Density, Ecomorphological Indices, and Soil Characteristics. *J. Ecol. Eng.* **2021**, *22*, 163–175. Available online: http://www.jeeng.net/Andean-Grassland-Species-Net-Aerial-Primary-Productivity-Density-Ecomorphological,138816,0,2.html (accessed on 13 September 2023). [CrossRef]
53. Kozlov, A.; Kozlova, M.; Skorik, N. A Simple Harmonic Model for FAPAR Temporal Dynamics in the Wetlands of the Volga-Akhtuba Floodplain. *Remote Sens.* **2016**, *8*, 762. [CrossRef]
54. Alexander, P.; Nielsen, D.L.; Nias, D. Response of wetland plant communities to inundation within floodplain landscapes. *Ecol. Manag. Restor.* **2008**, *9*, 187–195. [CrossRef]
55. Adjiski, V.; Zubíček, V. Continuous Monitoring of the Mining Activities, Restoration Vegetation Status and Solar Farm Growth in Coal Mine Region Using Remote Sensing Data. *Min. Rev.* **2023**, *29*, 26–41.
56. Radutu, A.; Vlad-Sandru, M.I. Review on the Use of Satellite-Based Radar Interferometry for Monitoring Mining Subsidence in Urban Areas and Demographic Indicators Assessment. *Min. Rev.* **2023**, *29*, 42–62.
57. Jin, K.; Wang, F.; Li, P. Responses of Vegetation Cover to Environmental Change in Large Cities of China. *Sustainability* **2018**, *10*, 270. [CrossRef]
58. Zedler, J.B.; Kercher, S. Causes and Consequences of Invasive Plants in Wetlands: Opportunities, Opportunists, and Outcomes. *Crit. Rev. Plant Sci.* **2004**, *23*, 431–452. [CrossRef]
59. Cui, L.; Li, G.; Liao, H.; Ouyang, N.; Li, X.; Liu, D. Remote Sensing of Coastal Wetland Degradation Using the Landscape Directional Succession Model. *Remote Sens.* **2022**, *14*, 5273. [CrossRef]
60. Cano, D.; Crispin, A.; Custodio, M.; Chanamé, F.; Peñaloza, R.; Pizarro, S. Space-time quantification of aboveground net primary productivity service supply capacity in high Andean bofedales using remote sensors. *J. Water Land Dev.* **2023**, *56*, 172–181.
61. Dong, S.K.; Wen, L.; Li, Y.Y.; Wang, X.X.; Zhu, L.; Li, X.Y. Soil-Quality Effects of Grassland Degradation and Restoration on the Qinghai-Tibetan Plateau. *Soil Sci. Soc. Am. J.* **2012**, *76*, 2256–2264. [CrossRef]
62. Wang, X.; Dong, S.; Yang, B.; Li, Y.; Su, X. The effects of grassland degradation on plant diversity, primary productivity, and soil fertility in the alpine region of Asia's headwaters. *Environ. Monit. Assess.* **2014**, *186*, 6903–6917. [CrossRef]
63. Quan, Q.; Nianpeng, H.; Zhen, Z.; Yunhai, Z.; Yang, G. Nitrogen enrichment and grazing accelerate vegetation restoration in degraded grassland patches. *Ecol. Eng.* **2015**, *75*, 172–177. [CrossRef]
64. Xu, X.; Hu, G.; Liu, X.; Lu, S.; Li, S.; Zhao, N. Impacts of nitrogen enrichment on vegetation growth dynamics are regulated by grassland degradation status. *Land Degrad. Dev.* **2021**, *32*, 4056–4066. [CrossRef]

65. Yu, J.; Wan, L.; Liu, G.; Ma, K.; Cheng, H.; Shen, Y.; Liu, Y.; Su, X. A Meta-Analysis on Degraded Alpine Grassland Mediated by Climate Factors: Enlightenment for Ecological Restoration. *Front. Plant Sci.* **2022**, *12*, 821954. [CrossRef]
66. Passera, C.B.; Borsetto, O.; Candia, R.J.; Stasi, C.R. Shrub control and seeding influences on grazing capacity in Argentina. *J. Range Manag.* **1992**, *45*, 480–482. [CrossRef]
67. Buchhorn, M.; Lesiv, M.; Tsendbazar, N.E.; Herold, M.; Bertels, L.; Smets, B. Copernicus Global Land Cover Layers—Collection 2. *Remote Sens.* **2020**, *12*, 1044. [CrossRef]
68. Neves, A.K.; Körting, T.S.; Fonseca, L.M.G.; Escada, M.I.S. Assessment of TerraClass and MapBiomas data on legend and map agreement for the Brazilian Amazon biome. *Acta Amaz.* **2020**, *50*, 170–182. [CrossRef]
69. Baeza, S.; Vélez-Martin, E.; De Abelleyra, D.; Banchero, S.; Gallego, F.; Schirmbeck, J.; Veron, S.; Vallejos, M.; Weber, E.; Oyarzabal, M.; et al. Two decades of land cover mapping in the Río de la Plata grassland region: The MapBiomas Pampa initiative. *Remote Sens. Appl. Soc. Environ.* **2022**, *28*, 100834. [CrossRef]
70. Cayo, E.Y.T.; Borja, M.O.; Espinoza-Villar, R.; Moreno, N.; Camargo, R.; Almeida, C.; Hopfgartner, K.; Yarleque, C.; Souza, C.M. Mapping Three Decades of Changes in the Tropical Andean Glaciers Using Landsat Data Processed in the Earth Engine. *Remote Sens.* **2022**, *14*, 1974. [CrossRef]